PROCEEDINGS OF ECOS 2026 - THE 39TH INTERNATIONAL CONFERENCE ON

EFFICIENCY, COST, OPTIMIZATION, SIMULATION AND ENVIRONMENTAL IMPACT OF ENERGY SYSTEMS

28 JUNE – 03 JULY, 2026, CONSTANTA, ROMANIA

Assessment of a Recuperated Ammonia Power Cycle for a Bimodal Nuclear Propulsion System

Alberto Tacchi [1,a], Elia Puccinelli [2,b], Guido Francesco Frate [1,c],
Angelo Pasini [2,d], and Lorenzo Ferrari [1,e]

[1] Dept. of Energy, System, Territory and Construction Engineering, Pisa, Italy,
[2] Dept. of Civil and Industrial Engineering, Pisa, Italy,
[a] alberto.tacchi@phd.unipi.it (CA), [b] elia.puccinelli@phd.unipi.it, [c] guido.frate@unipi.it,
[d] angelo.pasini@unipi.it, [e] lorenzo.ferrari@unipi.it.

Abstract:

Since the 1950s, nuclear reactors have been proposed for space use in both nuclear-thermal and nuclear-electric propulsion (NTP and NEP, respectively) systems. Bimodal architectures combine the high thrust of NTP with the high efficiency of NEP, using a single reactor. In the Bimodal Ammonia Nuclear Thermal and Electric Rocket (BANTER) concept, ammonia (NH_3) is used as a single-fluid system, serving as propellant for both NTP and NEP thrusters and as a working fluid for onboard power generation. Reactor heat is converted through a pump–turbine–generator chain; however, in a vacuum, the associated waste heat must be rejected radiatively, potentially leading to large radiators. Consequently, mission feasibility is closely tied to thermal-to-electric conversion efficiency and the corresponding heat-rejection duty. This paper evaluates the benefits and limitations of recuperation in a closed thermodynamic cycle for the conversion of the thermal power developed inside a nuclear bimodal propulsion system. Recuperation increases cycle efficiency and decreases the heat requirements for the heat source. Consequently, this reduces the heat rejection duty for the space radiators.

Results are shown in the form of operating maps, which depict the performance of the thermodynamic cycles considered for the identified configurations by varying the main parameters, namely the pump inlet and outlet pressures, the reactor outlet temperature, and the mass flow of the working fluid circulating in the cycle. The cycle is designed to generate a fixed electrical power output of 300 kWe.

Keywords:

Thermodynamics; Power conversion; Power Generation; Ammonia; Nuclear.

1. Introduction

BANTER is a bimodal system, which combines the high thrust of Nuclear Thermal Propulsion (NTP) with the high efficiency of the Nuclear Electric Propulsion (NEP), which enables the spacecraft to accomplish missions to the Moon, Mars and beyond. BANTER adopts a single working fluid – ammonia – for both propulsion and power generation. In this context, one of the main challenges is to design a power conversion system which is able to operate continuously both during NTP burns, the thermal power can peak at about 100 MW for short durations, and during NEP operation, where powers in the order of hundreds of kW are sustained for long periods. In NTP systems the nuclear fuel is the substance that provides heat via nuclear processes, while the propellant is the fluid that absorbs the heat and generates thrust. The working fluid, instead, is devoted to the conversion of the thermal power developed inside the reactor into electrical power. The fuel elements inside the reactor core produce heat and contain channels through which the propellant flows [1-3].

The present work highlights the main options for power conversion cycles operating with ammonia in bimodal nuclear space applications, and shows how recuperation increases system flexibility. First, recuperation increases efficiency, decreasing the thermal power requirement for the reactor, contributing to a smaller core and radiation shield, as well as reduced complexity [1]. Higher efficiency also reduces the waste heat load, but usually at the expense of a lower heat rejection temperature and larger radiator [2].

The challenges inherent to the design of a power conversion system for a nuclear-bimodal space platform are unique within the field and call for novel methodologies whose impact may extend beyond the space sector. The impact of BANTER is also expected to extend beyond space, reaching the energy sector – notably, its growing interest in NH_3 decomposition as a pathway to green hydrogen.

1.1. Review of existing cycles for space use

The literature offers many studies on the selection of the most suitable power conversion cycle in nuclear space applications. However, the selection of the most suitable power cycle depends on the power level that the spacecraft must generate, the operating temperatures, the scalability of the system to different power levels and the thermal-to-electric efficiency.

In a review concerning Nuclear Electric Propulsion (NEP) technologies [3], five power conversion technologies are compared. Dynamic systems, namely Brayton, Stirling and Rankine cycles are compared with two other static systems, namely Thermoelectric and Thermionic. Mason [3] demonstrated that dynamic systems offer a significant efficiency advantage over static systems.

In the 100 kWe class, Brayton systems have the lowest specific mass for NEP, offering high conversion efficiency (about 25%) and high power density turbomachinery. Brayton conversion also scales well over a wide range of power levels from 50 kW to 500 kW and beyond. The main drawback of the Brayton cycle is the large radiator size, which results from its relatively low heat-rejection temperature [3], [4], [5].

Rankine cycles provide the lowest mass option for MW-class power levels, with an expected maximum efficiency of about 20%. However, the two-phase working fluid introduces material issues, adding complexity and risk to the design.

Stirling cycles exhibit favourable specific mass for power levels less than about 40 kWe. As power levels increase, the Stirling system would require complex integration, and unfavourable mass scaling [3].

The thermodynamic cycle investigated in the present study can be operated with the fluid either in subcritical conditions, where phase transition and evaporation are present in the nuclear reactor passage, or with the fluid in supercritical conditions. Consequently, the performance of the analysed cycle is in-between Brayton and Rankine cycles from the literature.

2. Methodology

2.1. Model adopted for parametric analyses

A parametric thermodynamic trade-off study is carried out for a power conversion system with ammonia that may operate in a closed-loop mode, rejecting waste heat through radiators, or in an open (or hybrid) configuration, in which the turbine exhaust is only partially recirculated and can be used for propulsion- or propellant-management-related functions. The model quantifies thermal-to-electric efficiency and heat-rejection duty while accounting for turbomachinery performance, pressure losses, and heat-exchanger limitations. Regeneration is introduced via a recuperator that transfers heat from the turbine exhaust to the compressed flow upstream of the reactor heat addition.

Two possible configurations are analysed in the present study, both of them in closed cycle configuration, namely the configuration without recuperation, comprising a pump-reactor-turbine-radiator set, and a second identical one, with the addition of a regeneration at the turbine outlet, connected to the pump outlet to preheat the working fluid before entering the reactor.

The cycle is first implemented in Python, including fluidic and electrical components, and their interconnections. At this stage, the reactor and the radiator are modelled as constant heat sources, while the electric pump and turbine are represented as ideal machines with isentropic fixed efficiencies [6]. Fluid properties are obtained from the CoolProp library [7]. Depending on the case, either a fixed (unit) mass flow rate or a specified electrical power output can be imposed to explore different design options. A parametric analysis is implemented by varying the main cycle parameters. Cycle efficiency, heat input and rejection, net power produced are evaluated varying the outlet reactor temperature, the outlet and inlet pump pressures.

2.1.1. Closed cycle without regeneration

This section outlines the procedure adopted for the parametric analysis of the power generation (PG) cycle without regeneration. The cycle is closed and includes the nuclear reactor, pump, turbine, and radiators, as shown in Figure 2.1. Python code was developed to evaluate either the net electrical power output produced by the cycle for a fixed working-fluid mass flow rate; or the working-fluid mass flow rate required to generate a prescribed net electrical power output. The cycle efficiency is defined as:

$$\eta = \frac{\dot{W}_{turbine} - \dot{W}_{pump}}{\dot{Q}_{input}} = \frac{\dot{W}_{net}}{\dot{Q}_{input}} \tag{1}$$

Where $\dot{Q}_{input}$ is the thermal power added to the working fluid while it flows through the nuclear reactor, and $\dot{W}_{net}$ is the net electrical power produced by the cycle. The parametric analysis is initialized using the reference cycle conditions of Table 2.1 below. The initial setting, and the required target electrical power level, are based on preliminary estimations and system requirements of the BANTER system [8], [9].

Table 2.1. Setting for cycle without regenerator.

Setting of Cycle without recuperation		
Pump inlet pressure	[bar]	10
Pump inlet subcooling	[K]	5
Reactor pressure ratio	[-]	0.9
Radiator pressure ratio	[-]	0.9
Reactor outlet temperature	[K]	700
Net electrical power produced	[kWe]	300

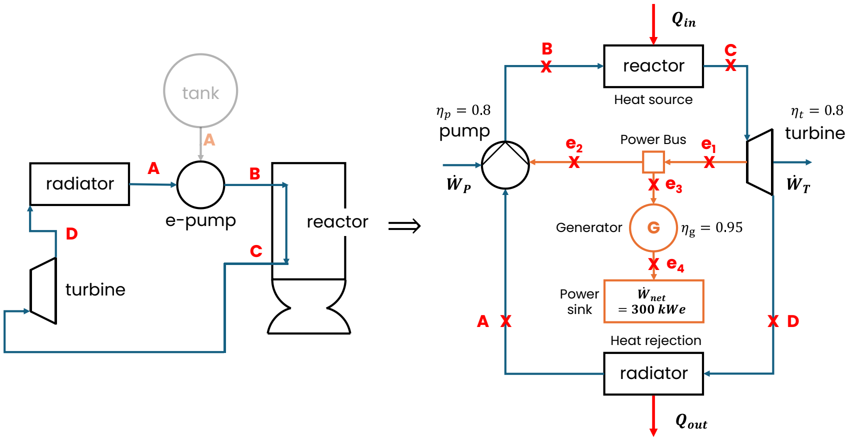

Figure 2.1. Schematics of the PGS without regeneration: actual system (left) and adaptation for parametric analysis (right). Blue lines indicate hydraulic ducts; orange lines electrical connections.

These reference conditions were derived from previous system analyses and are used as the starting point for the present study. The pump inlet conditions provide a degree of subcooling to mitigate cavitation likelihood. Depending on the analysis objective, either a unit (1 kg/s) fixed mass flow rate or a target net electrical power output can be imposed. Pressure-loss factors across the reactor and radiators were assumed based on reasonable preliminary estimates; further refinement will be supported by (i) detailed thermo-hydraulic analyses of the reactor cooling channels and (ii) a dedicated heat-transfer analysis of the radiator. An allowable turbine inlet temperature—corresponding to the reactor outlet temperature—is also assumed. Reasonable values for isentropic pump and turbine efficiencies are used, with $\eta_{pump} = \eta_{turbine} = 0.8$.

The parametric analysis spans over reactor outlet temperatures T_C ranging between 500 and $1000\ K$, pump outlet pressures between 50 and $150\ bar$, as shown in the pressure-specific enthalpy diagram of Figure 2.2 below. Pump inlet pressure can vary between 10 and $30\ bar$, however it is not shown in the figure for clarity purposes.

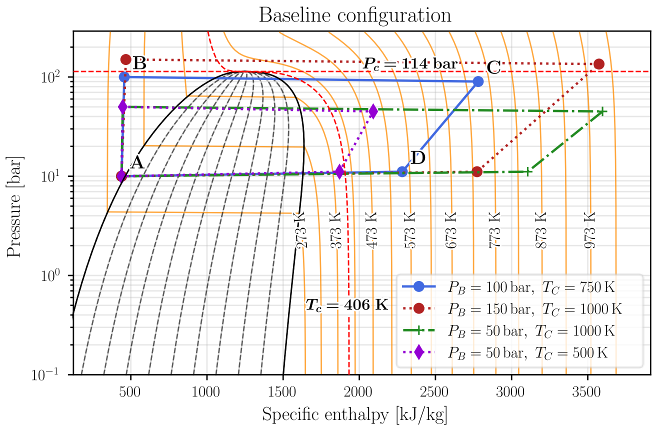

Figure 2.2. Pressure/Specific Enthalpy diagram: domain investigated in the parametric analysis of the baseline cycle without regenerator.

2.1.2. Closed cycle with regeneration

The power conversion cycle may be equipped with a regenerator inserted at the turbine outlet, which takes advantage of some heat available in the turbine exhaust to pre-heat the working fluid on the cold side of the regenerator, before entering the nuclear reactor, as shown in Figure 2.3 below.

The same setting of the closed cycle without recuperation is adopted, as in Table 2.1. Reasonable estimates of the cold and hot side pressure ratios are added, namely $pr_{regenerator}^{cold} = pr_{regenerator}^{hot} = 0.98$. A pinch-point analysis was implemented to guarantee a minimum pinch temperature difference between the hot and cold streams of about $\Delta T_{pinch} = 15\ K$, which is imposed at the cold side inlet/hot side outlet of the regenerator (points B-F of Figure 2.3) [10]. The same ranges adopted for the parametric analysis of the closed cycle without recuperation are used here for reactor outlet temperature, pump outlet and inlet pressures. The corresponding pressure-specific enthalpy diagram is shown in Figure 2.4 below.

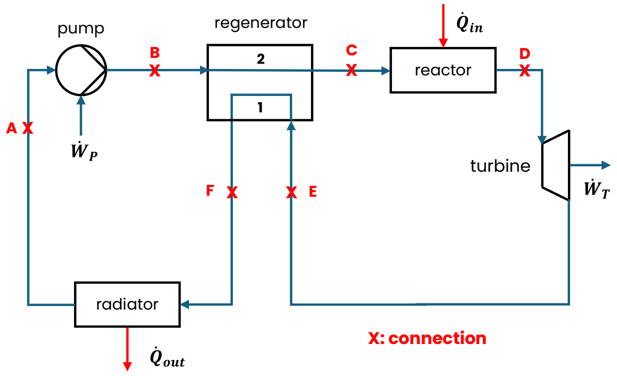

Figure 2.3. Schematic of the PGS with regeneration. Blue lines indicate hydraulic ducts.

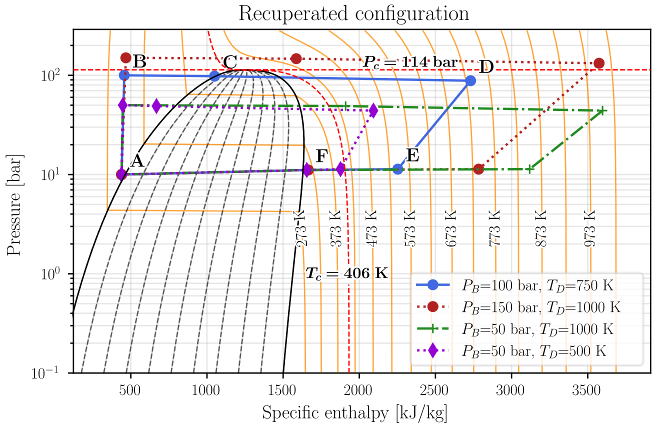

Figure 2.4. Pressure/Specific Enthalpy diagram: domain investigated in the parametric analysis of the cycle without regenerator.

3. Results

The results of the parametric analysis made on the closed cycle without and with regeneration are shown in the present section. Cycle efficiency and net power produced for a unit mass-flow rate are represented in maps that show their trends over the investigated space [11]. The parametric analysis ranges are shown in Table 3.1.

Table 3.1. Parameters and corresponding ranges used in the cycle parametric analysis.

Parameter space investigated in the parametric analysis		
Reactor outlet temperature	[K]	[500, 1000]
Pump inlet pressure	[bar]	[10, 30]
Pump outlet pressure	[bar]	[50, 150]

3.1. Closed cycle without recuperation

Results for the closed cycle without the regenerator are shown in Figure 3.1 and Figure 3.2 below, respectively depicting the thermal-to-electric conversion efficiency of the cycle and the net electrical power produced by the cycle for a fixed unit mass-flow rate.

The thermal-to-electric efficiency predicted for the non-recuperated cycle spans 13 – 25 % at $P_A = 10\ bar$ (Figure 3.1-left) and decreases to 3 – 16 % when P_A is raised to 30 bar (Figure 3.1-right). At a higher pump inlet pressure the working fluid enters the reactor closer to its critical point, reducing the available expansion across the turbine for a given heat input, reducing the cycle efficiency. Conversion efficiency is in line with literature: the proposed cycle gives a conversion performance between a Rankine cycle, whose expected efficiency ranges between 10 and 12%, and a Brayton cycle, whose expected efficiency ranges between 20 and 22% [3], [12].

The net electrical power output $\dot{W}_{net}$, with a fixed mass flow $\dot{m} = 1\ kg/s$, decreases as the cycle becomes less efficient with increasing pump inlet pressure p_A. The specific net power per unit mass-flow can reach 730 kWe for the most efficient cycle, operating at a reactor outlet temperature of 1000 K, a pump inlet pressure of 10 bar, and a pump outlet pressure of 150 bar (Figure 3.2, left). However, the net power can also become lower than the required power level, reaching 45 kWe for the least efficient cycle, operating at the lowest reactor outlet temperature of 500 K, a pump inlet pressure of 30 bar, and a pump outlet pressure of 50 bar (Figure 3.2, right).

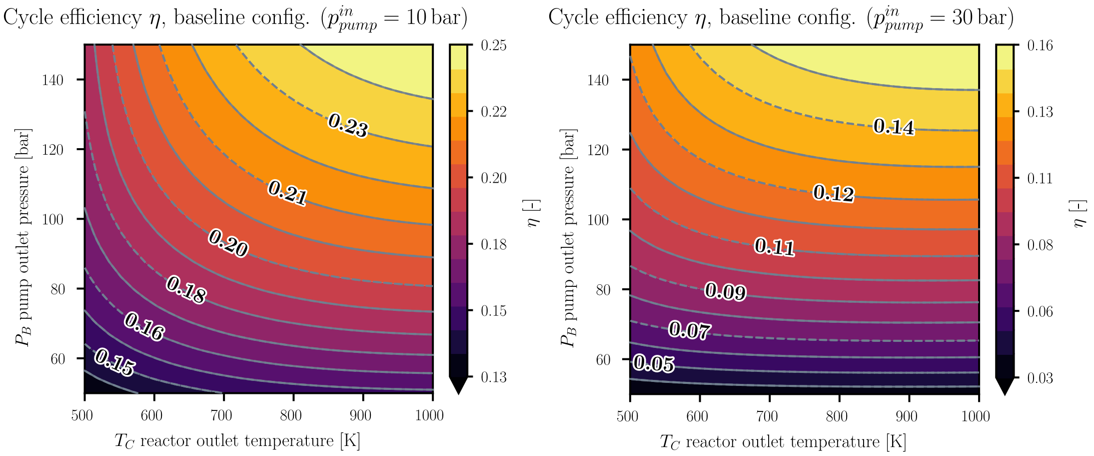

Figure 3.1. Efficiency over the investigated space for pump inlet pressures of 10 bar (left) and 30 bar (right), closed cycle without regeneration.

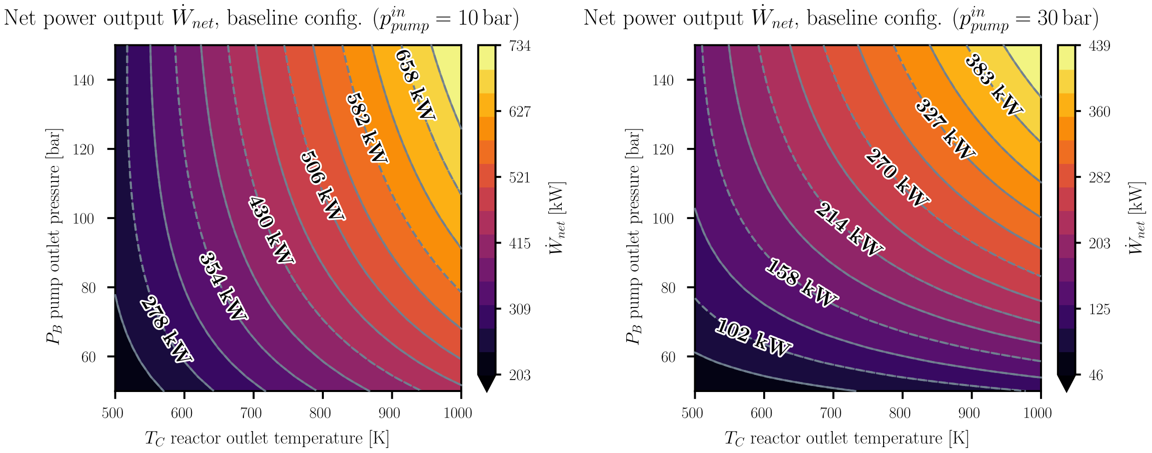

Figure 3.2. Net electrical power produced over the investigated space for a fixed unit mass-flow rate for pump inlet pressures of 10 bar (left) and 30 bar (right), closed cycle without recuperation.

3.2. Closed cycle with recuperation

Results for the closed cycle with the regenerator are shown in Figure 3.3 and Figure 3.4 below, respectively depicting the thermal-to-electric conversion efficiency of the cycle and the net electrical power produced by the cycle for a fixed unit mass-flow rate.

Efficiency varies between 15 and 38% for the case with a pump inlet pressure of 10 bar (Figure 3.3-left), and between 4 and 30% for the case with a pump inlet pressure of 30 bar (Figure 3.3-right). The case with the regenerator provides a greater margin to increase the pump inlet pressure P_A: this can help to reduce the radiator size. In fact, less heat needs to be added across the reactor, and a higher saturation temperature at the radiator – and hence a smaller radiator area – can be tolerated without compromising the power conversion performance.

The specific net power per unit mass flow can reach 724 kWe for the most efficient cycle, operating at a reactor outlet temperature of 1000 K, a pump inlet pressure of 10 bar, and a pump outlet pressure of 150 bar (Figure 3.4, left). However, the net power can also become lower than the required power level, reaching 40 kWe for the least efficient cycle, operating at the lowest reactor outlet temperature of 500 K, a pump inlet pressure of 30 bar, and a pump outlet pressure of 50 bar (Figure 3.4, right). The recuperated cycle yields a slightly lower specific power output than the baseline. This influences the required mass flow, which is slightly higher for the recuperated cycle. However, while the decrease in the specific power is relatively modest, the gain in the reduction of the required thermal power input and output is significant, as shown in Section 3.3.

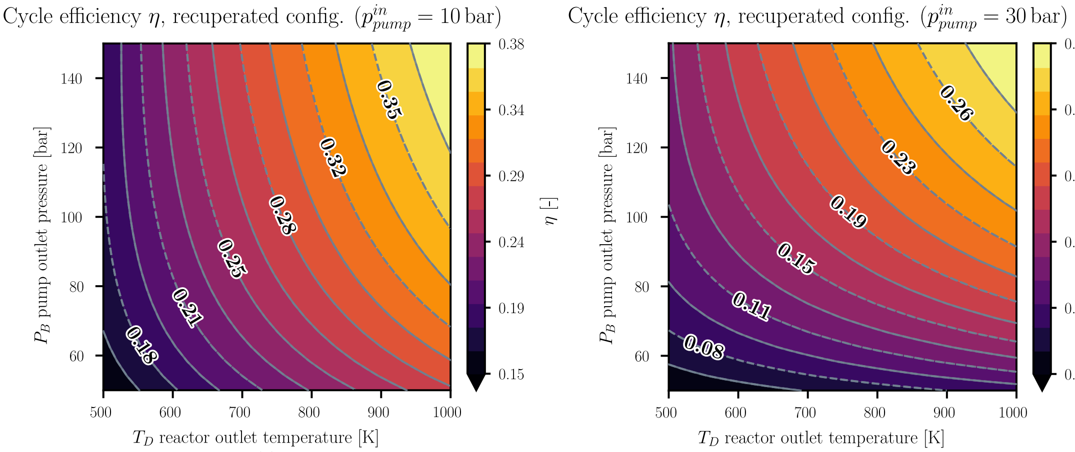
Cycle efficiency η, recuperated config. ($p_{pump}^{in} = 10\,\mathrm{bar}$)

Cycle efficiency η, recuperated config. ($p_{pump}^{in} = 30\,\mathrm{bar}$)

Figure 3.3. Efficiency over the investigated space for pump inlet pressures of 10 bar (left) and 30 bar (right), closed cycle with regenerator.

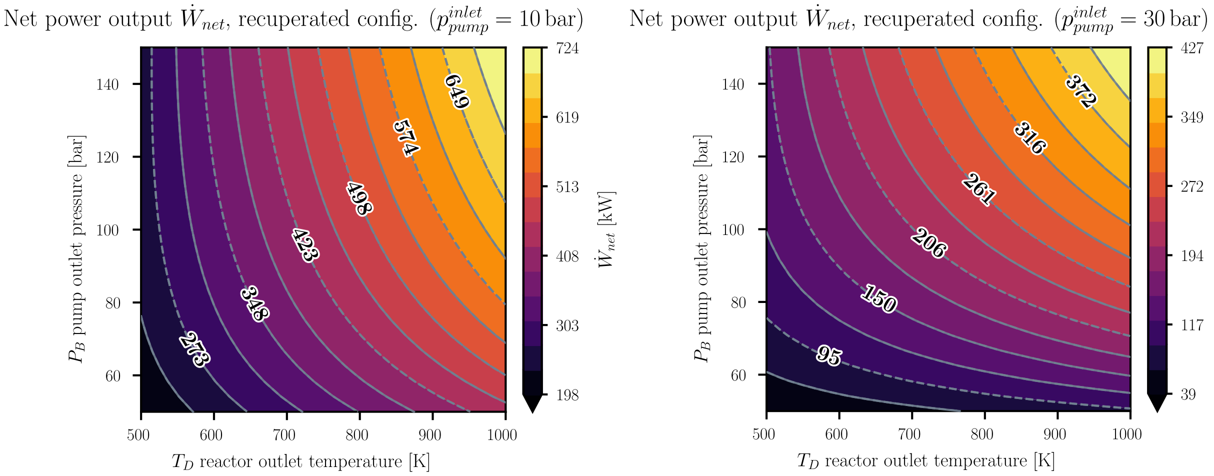
Net power output $\dot{W}_{net}$, recuperated config. ($p_{pump}^{inlet} = 10\,\mathrm{bar}$)

Net power output $\dot{W}_{net}$, recuperated config. ($p_{pump}^{inlet} = 30\,\mathrm{bar}$)

Figure 3.4. Net electrical power over the investigated space for a fixed unit mass-flow rate for pump inlet pressures of 10 bar (left) and 30 bar (right), closed cycle with regenerator.

3.3. Operating maps: specific heat input and output

Operating maps for heat power input of nuclear reactor and heat rejection duty for radiators with mass flow rate are shown in the present section. The selected outlet pump pressure range is raised between 90 and 150 bar, and reactor outlet temperature between 600 and 1000 K, where the cycle performs better. The pump inlet pressure can be increased from 10 to 30 bar in order to decrease the latent heat and increase the saturation temperature of the working fluid that must be condensed in the radiators: this strategy enables the reduction of the radiator size. Since the radiator size is strongly influenced by its operating temperature, an increase in the saturation temperature results in a decrease of the radiator size. Therefore, it is important to evaluate the consequent heat rejection duty of such an approach.

In the operating maps of Figure 3.5, the reactor heat input is shown against the cycle mass flow rate, and in maps of Figure 3.6 the heat rejection output is shown with the working fluid mass flow rate. Here the objective is to generate the required power level, that is 300 kWe, using the minimum heat power from the source, decreasing as much as possible the heat rejection duty, and to minimise the required mass flow rate, which can be used for other purposes. It is worth noting that the final thermodynamic cycle configuration might be a hybrid version between an open and a closed cycle. In this view, it is important to limit the use of ammonia, since the open-cycle configuration would limit the mission duration. Even if In-Situ Resource Utilization (ISRU) is possible on the Lunar and Mars surfaces [13], refuelling in low-gravity environments, such as in space, can be challenging. Therefore, it is recommended to limit as much as possible the consumption of ammonia in hybrid- and open-cycle configurations.

The case without recuperation (Figure 3.5-left; Figure 3.6-left) shows that the most efficient cycle, with the maximum values of the pump outlet pressure and reactor outlet temperature of 150 bar and 1000 K, enables the heat input to be minimised to 1270 kW, and the heat output to 954 kW, with a mass-flow of $0.41\ kg/s$.

The introduction of the regenerator has a significant effect on the reduction of both the thermal heat input required for the nuclear reactor, as shown in Figure 3.5, right, and the heat rejection duty, as shown in Figure 3.6-right. The higher efficiency of the cycle makes it possible to obtain the same power level of 300 kWe by taking less thermal power from the reactor, and reducing the heat rejection duty. Here, the most efficient cycle can minimise the thermal input to 824 kWt and the heat rejection duty to 508 kWt, with a mass flow rate of $0.41\ kg/s$.

Overall, for both cases, with and without recuperation, the rise in the pump inlet pressure P_A limits the minimum heat input required for the reactor and the minimum heat rejection duty to higher levels, since the cycle is less efficient. Results for both configurations are gathered in Table 3.2 and Table 3.3.

Table 3.2. Optimal points at pump inlet pressures of 10 and 30 bar, baseline configuration.

Baseline configuration, optimal points	Pump inlet pressure	
	10 bar	30 bar
Heat input	1270 kWt	1985 kWt
Heat output	954 kWt	1670 kWt
Mass flow rate	0.41 kg/s	0.68 kg/s

Table 3.3. Optimal points at pump inlet pressures of 10 and 30 bar, recuperated configuration

Recuperated configuration, optimal points	Pump inlet pressure	
	10 bar	30 bar
Heat input	824 kWt	1045 kWt
Heat output	508 kWt	728 kWt
Mass flow rate	0.41 kg/s	0.70 kg/s

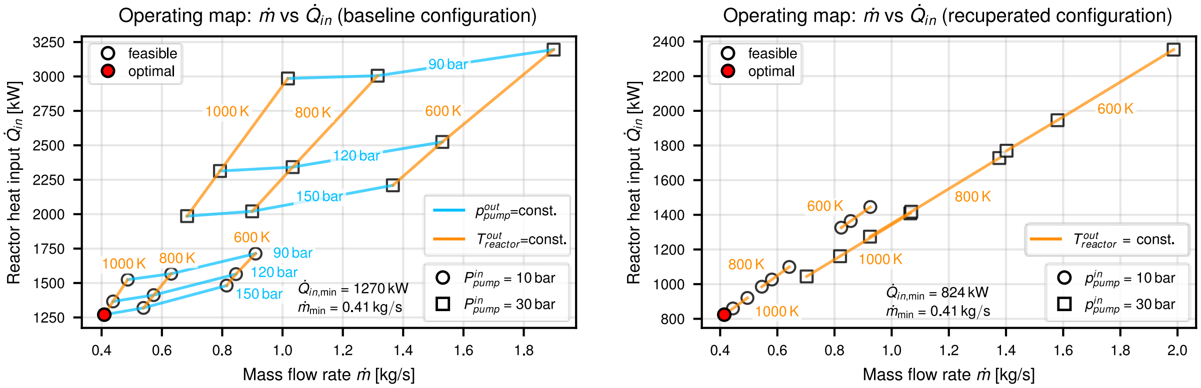

Figure 3.5. Operating maps for the closed cycles without (left) and with (right) regenerator: heat input power from the nuclear reactor in [kW] vs cycle mass flow in [kg/s]. Pump outlet pressure P_B from 90 to 150 bars, reactor outlet temperatures T_C (or T_D) between 600 and 1000 K. Configurations discretized based on pump inlet pressure P_A values of 10 and 30 bar. Lines with constant pump outlet pressure P_B and reactor outlet temperature T_C are shown in light blue and orange, respectively.

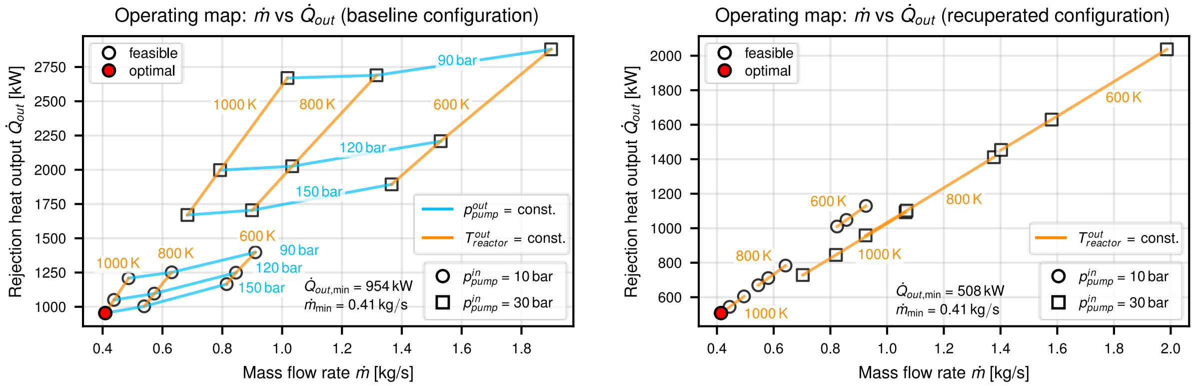

Figure 3.6. Operating maps for the closed cycles without (left) and with (right) regenerator: heat rejection output power in [kW] vs cycle mass flow in [kg/s]. Pump outlet pressure P_B from 90 to 150 bars, reactor outlet temperatures T_C (or T_D) between 600 and 1000 K. Configurations discretized based on pump inlet pressure P_A values of 10 and 30 bar. Lines with constant pump outlet pressure P_B and reactor outlet temperature T_C are shown in light blue and orange, respectively.

4. Conclusions

The design of a power generation cycle for a bimodal nuclear propulsion system must ensure optimal performance while remaining as independent as possible from the operating constraints of the nuclear reactor. This study demonstrated that integrating a recuperator into the thermodynamic cycle significantly increases conversion efficiency, by about 14%, and system flexibility. By pre-heating the working fluid before it enters the reactor, the required thermal power input from the core is reduced by approximately 35%, which in turn enables a smaller reactor core and radiation shield. In addition, the thermal power to be rejected is reduced by about 47 %. Although this reduction in waste heat is substantial, the corresponding decrease in radiator size may be less pronounced due to the limitations imposed by the condensation temperature. Ultimately, the use of recuperation in the BANTER power conversion cycle proves to be a key design strategy, offering a more reliable architecture while significantly alleviating the thermo-hydraulic constraints for the cooling channels of the reactor.

Acknowledgements

The project leading to this paper has received funding from the European Union's research and innovation programme under agreement No 101186520. BANTER, Bimodal Ammonia Nuclear Thermal and Electric Rocket.

European Innovation Council
Funded by the European Union

BANTER

Nomenclature

Math symbols

h	Specific enthalpy, kJ/kg
$\dot{m}$	Mass flow rate, kg/s
p	Pressure, bar
P_A	Pump inlet pressure, bar
P_B	Pump outlet pressure, bar
P_C	Critical pressure, bar
$\dot{Q}_{in}$	Thermal power added (heat input), kW or kWt
$\dot{Q}_{out}$	Waste heat rejected (heat output), kW or kWt
T	Temperature, K
T_C	Reactor outlet temp., K
T_D	Reactor outlet temp. (recuperated cycle), K
ΔT_{pinch}	Minimum pinch temperature difference, K
$\dot{W}_{net}$	Net electrical power produced, kW or kWe
$\dot{W}_P$	Pump power, kW

$\dot{W}_T$ *or* $\dot{W}_{turbine}$: Turbine power, kW

Greek Symbols

η	Thermal-to-electric conversion efficiency

η_p or η_{pump}: Isentropic pump efficiency

η_t or $\eta_{turbine}$: Isentropic turbine efficiency

Abbreviations / Acronyms

BANTER: Bimodal Ammonia Nuclear Thermal and Electric Rocket

NEP: Nuclear Electric Propulsion

NTP: Nuclear Thermal Propulsion

PG / PGS: Power Generation System

NH_3: Ammonia

References

[1] A. Pasini, V. Giusti, D. E. Puccinelli, and G. Belli, 'Radiation Shielding and Orbital Safety Strategies for a Space Nuclear Propulsion System', Master thesis, University of Pisa, Pisa, 2025. [Online]. Available: https://etd.adm.unipi.it/t/etd-07022025-153339/

[2] B. Sondelski and G. Nellis, 'Mass optimization of a supercritical CO2 Brayton cycle with a direct cooled nuclear reactor for space surface power', *Appl. Therm. Eng.*, vol. 163, p. 114299, Dec. 2019, doi: 10.1016/j.applthermaleng.2019.114299.

[3] L. S. Mason, 'Power technology options for nuclear electric propulsion', in *IECEC '02. 2002 37th Intersociety Energy Conversion Engineering Conference, 2002.*, Washington, WA, USA: IEEE, 2004, pp. 114–121. doi: 10.1109/IECEC.2002.1391989.

[4] E. Wood and L. D. Thomas, 'Nuclear Thermal Propulsion Engine Minimally-Intrusive Power Generation Alternatives', in *AIAA Propulsion and Energy 2021 Forum*, VIRTUAL EVENT: American Institute of Aeronautics and Astronautics, Aug. 2021. doi: 10.2514/6.2021-3605.

[5] A. J. Juhasz and H. S. Bloomfield, ‘Development of Lightweight Radiators for Lunar Based Power Systems’, presented at the International Conference On Environmental Systems, Friedrichshafen, Germany, Jun. 1994, p. 941327. doi: 10.4271/941327.

[6] P. Rachov, ‘ELECTRIC FEED SYSTEMS FOR LIQUID PROPELLANT ROCKET ENGINES’.

[7] K. Gao, J. Wu, I. H. Bell, A. H. Harvey, and E. W. Lemmon, ‘A Reference Equation of State with an Associating Term for the Thermodynamic Properties of Ammonia’, *J. Phys. Chem. Ref. Data*, vol. 52, no. 1, p. 013102, Mar. 2023, doi: 10.1063/5.0128269.

[8] J. Grill, G. Becatti, G. Herdrich, E. Puccinelli, and A. Pasini, ‘Integrating Mission and System Analyses in the BANTER Project for Nuclear Bimodal Propulsion’, in *IAF Space Propulsion Symposium*, Sydney, Australia: International Astronautical Federation (IAF), 2025, pp. 1106–1120. doi: 10.52202/083090-0122.

[9] E. Puccinelli, V. Giusti, J. Grill, G. Becatti, G. Herdrich, and A. Pasini, ‘Definition of Requirements and System Engineering of the Innovative Bimodal Ammonia Nuclear Thermal and Electric Rocket (BANTER)’, in *IAF Space Propulsion Symposium*, Sydney, Australia: International Astronautical Federation (IAF), 2025, pp. 836–849. doi: 10.52202/083090-0089.

[10] G. F. Nellis and S. A. Klein, *Heat transfer*, 1. paperback ed. Cambridge: Cambridge University Press, 2012.

[11] G. C. Bucher, ‘An Analysis of the Thermodynamic Cycle and Possible Working Fluids for a Space Heat Rejection System -’. Marshall Space Flight Center. Huntsville, Alabama, Aug. 1960. [Online]. Available: https://apps.dtic.mil/sti/tr/pdf/ADB182385.pdf#:~:text=Within%20%2Dthe%20next%20few%20years%2C%20nuclear%20reactor,Carnot%20thermodynamic%20cycle%20is%20analyzed%20to%20de%2D.

[12] H. M. Dieckamp, ‘NUCLEAR SPACE POWER SYSTEMS.’, AI-Memo--7585, 4505769, Jan. 1967. doi: 10.2172/4505769.

[13] D. Nikitaeva and L. D. Thomas, ‘Preliminary Results for In-Situ Alternative Propellants for Nuclear Thermal Propulsion’, *Nucl. Technol.*, vol. 208, no. sup1, p. 10, Dec. 2022, doi: 10.1080/00295450.2021.2021768.